IEEE Access
Multidisciplinary | Rapid Review | Open Access Journal

Received March 19, 2019, accepted April 6, 2019, date of publication April 24, 2019, date of current version May 14, 2019.

Digital Object Identifier 10.1109/ACCESS.2019.2912983

An Improved IMM Algorithm Based on STSRCKF for Maneuvering Target Tracking

BO HAN[1], HANQIAO HUANG[2], LEI LEI[3], CHANGQIANG HUANG[1], AND ZHUORAN ZHANG[1]

[1]Aeronautics Engineering College, Air Force Engineering University, Xi'an 710038, China
[2]Unmanned System Research Institute, Northwestern Polytechnical University, Xi'an 710072, China
[3]Electric Power Research Institute, State Grid Shaanxi Electric Power Company, Xi'an 710021, China

Corresponding author: Hanqiao Huang (huanghanqiao@nwpu.edu.cn)

This work was supported in part by the National Natural Science Foundation of China, under Grant 61601505.

ABSTRACT To overcome the IMM algorithm is easy divergence and low tracking accuracy when dealing with complex maneuvering situations, this paper proposes an improved interactive multiple model strong tracking square room cubature Kalman filter (IIMM-STSRCKF) algorithm under the idea of real-time dynamic adjustment of gain matrix and transition probability matrix. The algorithm has been improved in two aspects: on the one hand, the algorithm uses the idea of a strong tracking filter to deduce a new method for time-varying fading factor and introduce it into the square root of the state error covariance matrix of the SRCKF, which improves the tracking accuracy for strong maneuver; on the other hand, the probability difference between two consecutive time points in the IMM submodel is used to adjust the Markov probability transfer matrix to adaptively improve the switching speed of the submodel and the rationality of the allocation. By comparing with IMM-CKF algorithm by maneuvering target tracking case and results show that the IIMM-STSRCKF algorithm has better tracking performance in nonmaneuvering, weak maneuvering, and strong maneuvering cases.

INDEX TERMS Complex maneuvering, IMM, SRCKF, strong tracking filter.

I. INTRODUCTION

Maneuvering target tracking is a typical nonlinear filtering process and has become a major area of interest in the field of state estimation and information fusion, having been widely used in radar tracking, navigation control, guidance and other fields [1]. Difficulties in this field primarily arise from two aspects: the design of the tracking model and the selection of a nonlinear filter [2].

The tracking model problem primarily studies whether the state model of the tracking system conforms to the real-time motion model of the target. Due to the complexity and randomness of target motion, it is difficult to completely describe different maneuvering situations in a single model, which leads to a mismatch between the state model and the actual movement of the target. Therefore, the tracking effect is unsatisfactory. The interactive multiple model (IMM) [3], [5] can solve this problem; it maps the target motion model into a number of known model sets, with each model filter working in parallel. A Markov probability transfer matrix is used to obtain interactions and switching among different submodels. Finally, the algorithm performs data fusion on the target state filter estimation obtained by each model filter to obtain the system parameter estimation [6], [7].

[8] studies the stability of IMM algorithm from the mathematical theorem, and proposes the exponential stability for a class of Markov jump linear systems. It proves that IMM algorithm has good performance in various low-cost computing application. IMM filter based on steady-state filter is proposed, and filter uses adaptive algorithm to determine the target revisit time, which improves the prediction accuracy and reduces the computational load [3]. [9] constructs a position estimation algorithm by using the basic IMM of a jump Markov system with two independent switching parameters, and prove the effectiveness of the IMM algorithm in the field of target tracking.

The Markov transition probability matrix determines the interaction and switching between models; thus, it strongly affects the tracking performance of the IMM algorithm [10]. In the standard IMM algorithm, the Markov probability transfer matrix is artificially set to a fixed diagonally dominant matrix. However, due to the strong randomness and

The associate editor coordinating the review of this manuscript and approving it for publication was Feng Xia.

high dynamics of maneuvering targets, as well as the uncertainty of prior knowledge, the fixed diagonally dominant matrix often leads to a lag in the algorithm model switching, which leads to the deterioration of the tracking effect [11]. Therefore, a method for adaptively adjusting the Markov transition probability matrix online is a key issue for improving the tracking performance of the IMM algorithm [12].

Filter selection is another key factor in the IMM algorithm. The performance of the filter directly affects the tracking effect of the IMM algorithm. The Kalman filter (KF) is a classical linear filtering method [13], [14] that has been applied to signal processing and target tracking. Even though the measurement model of the maneuvering target tracking tends to have strong nonlinearity and its state space has obvious nonlinearity, the KF can only deal with a linear time-invariant system; thus, it is necessary to select an appropriate nonlinear filter. The extended Kalman filter (EKF) [15], [16] solves the nonlinear filtering problem by locally linearizing the nonlinear problem through a Taylor expansion. The approximate accuracy of the EKF for a nonlinear function is first order, and the Jacobian matrix must be calculated, which leads to unsatisfactory filtering accuracy. Juiler et al. proposed a deterministic sampling approximate Gaussian filtering algorithm based on an unscented transform (UT)—unscented KF (UKF) algorithm [17], which does not require the Jacobian matrix to be solved, has no derivative requirement for the state transfer function or the measurement function of nonlinear systems, and whose accuracy can reach at least the third order. However, when dealing with high-dimensional systems, the algorithm must select reasonable parameters to achieve a higher precision.

Arasaratnam I et al. proposed the cubature KF (CKF) algorithm [18], which uses spherical-radial information to obtain the cubature criterion and approximates the probability integral via Bayesian filtering. The CKF algorithm further optimizes the sampling point selection method and weight distribution strategy in the UKF algorithm and solves the problem in which the filtering effect of the UKF algorithm is unsatisfied in high-dimensional systems. Therefore, the nonlinear approximation of the CKF algorithm is better than that of the UKF.

CKF not only overcomes the application limitations of EKF and UKF in strong nonlinear system, but also has higher filtering accuracy than central difference Kalman filter (CDCKF) and particle filtering [19], further, the error covariance non-positive and asymmetry problems caused by rounding errors and other factors are further solved. Reference [20] proposes the apply the matrix QR decomposition to the update error covariance matrix, thus forming the SRCKF algorithm. SRCKF was widely used in navigation and positioning [21], target tracking [22], robotics [23], aerospace positioning [24] and other fields.

Chen et al. [9], [25] proposed combining the IMM with the CKF to design an algorithm for maneuvering target tracking and demonstrated that the IMM-CKF has a better tracking effect than the IMM-UKF algorithm, but the CKF algorithm can appear asymmetric or have nonpositive values in the covariance matrix in the process of iteration, which causes the estimation accuracy to decline and interrupts the iteration process. CKF is limited by the influence of the third-order volume rule, and the estimation accuracy is still limited in some filtering problems. In order to improve the filter precision of CKF, Swati and Shovan [26] are based on the spherical-phase diameter rule and the Gauss-Laguerre quadrature rule (CQKF), and analyze the relationship between CQKF and CKF. It is pointed out that CKF is a special form of CQKF in the selection of first-order Gauss-Laguerre integration points [27]. Jia and Xin [28], [31] from Columbia University –Missouri State University analyzed the volume rule that can obtain the accuracy of arbitrary order estimation, and proposed a high-order Cuban Kalman Filter (HCKF) method with more volume points. Meanwhile, They focus on the fifth-order volume Kalman filter and show the filter accuracy is similar to the Gaussian Hermititian filter (GHQF) [32]. Although the calculation is much smaller that GHQF, but it is much larger that CKF, so it is not conducive to tracking high-speed target [28].

The strong tracking filter is an improved extended EKF, which can significantly improve the speed of convergence and tracking when large and sudden maneuver changes occur while the measurement error is unknown. STF also reduces sensitivity to initial conditions [19], [33].To improve the filtering effect of the CKF, Arasaratban and Haykin [18] further proposed a square root CKF (SRCKF) to ensure the advantages of a positive covariance matrix. However, the CKF and SRCKF both have poor robustness, precision and tracking effects when the target state mutation or the model matching is not accurate.

Aimed at the above problems, this paper proposes an Improved IMM strong tracking SRCKF (IIMM-STSRCKF) maneuvering target tracking algorithm [19], [20] based on the IMM algorithm and a strong tracking filter (STF). The algorithm deduces a new equivalent method for evaluating the time-varying fading factor, which is introduced into the square root of the state prediction error covariance matrix. This approach improves the tracking ability of the SRCKF algorithm for a maneuvering target with state mutation. In addition, the Markov probability transfer matrix is adjusted in real time using posterior information on the difference in conditional probability between two consecutive time points in the model, which effectively improves the filtering accuracy. Simulation results show that the proposed IIMM-STSRCKF algorithm has a superior tracking performance.

The remainder of this paper is organized as follows. Section 2 and Section3 provides a brief overview of the principles and structure of the SRCKF and IMM-SRCKF respectively. Section 4 details the working methodology of the Adaptive STSRCKF algorithm. Section 5 introduces the Modified Markov probability matrix of the IMM algorithm in detail. Section 6 describes the simulation experiments.

Section 7 summarizes the paper and describes directions for future research.

II. SRCKF ALGORITHM

The SRCFK algorithm is based on the idea of the square root in the KF. QR decomposition is introduced in the CKF algorithm, and the square root of the covariance matrix is used instead of the covariance matrix to recursively update the algorithm; hence, this method reduces the complexity of the original operation and improves the filter efficiency. Meanwhile, the numerical instability caused by rounding errors is avoided, and the filter accuracy and stability are improved. The QR decomposition process in the SRCKF algorithm is as follows:

The error covariance matrix is $\boldsymbol{P} = \boldsymbol{A}\boldsymbol{A}^T$, and the QR decomposition is introduced. Then $\boldsymbol{A}^T = \boldsymbol{Q}\boldsymbol{R}$, where Q is the orthogonal matrix, and R is the upper triangular matrix.

$$\boldsymbol{P} = \boldsymbol{A}\boldsymbol{A}^T = (\boldsymbol{Q}\boldsymbol{R})^T\boldsymbol{Q}\boldsymbol{R} = \boldsymbol{R}^T\boldsymbol{Q}^T\boldsymbol{Q}\boldsymbol{R} = \boldsymbol{R}^T\boldsymbol{R} = \boldsymbol{S}\boldsymbol{S}^T \quad (1)$$

where $\boldsymbol{S} = Tria\,[\boldsymbol{A}]$ is the square root of the error covariance, which can be obtained by Cholesky decomposition.

$\boldsymbol{S}_{\boldsymbol{Q}}$ and $\boldsymbol{S}_{\boldsymbol{R}}$ are defined as the square root of the process noise and measurement noise variance, respectively. For a constant speed tracking model, the specific steps of the SRCKF algorithm are summarized as follows:

Step 1: Initialization

The state initial mean is $\hat{\boldsymbol{X}}_0$, the error covariance is $\boldsymbol{P}_0$, and $\boldsymbol{P}_0$ is decomposed by Cholesky decomposition to obtain the following the square root:

$$\boldsymbol{S}_0 = chol(\boldsymbol{P}_0)^T \quad (2)$$

Step 2: Time update

Evaluate the cubature points $(i = 1, 2, \cdots, m)$

$$\boldsymbol{X}_{i,k-1} = \boldsymbol{S}_{k-1}\boldsymbol{\xi}_i + \hat{\boldsymbol{X}}_{k-1} \quad (3)$$

Evaluate the propagated cubature points

$$\boldsymbol{X}^*_{i,k|k-1} = \boldsymbol{\Phi}_{k|k-1}\boldsymbol{X}_{i,k-1} \quad (4)$$

Estimate the predicted state

$$\boldsymbol{X}_{k|k-1} = \sum_{i=1}^{m} \omega_i \boldsymbol{X}^*_{i,k|k-1} \quad (5)$$

Calculate the square root of the state prediction error covariance

$$\boldsymbol{S}_{k|k-1} = Tria\left(\left[\begin{array}{cc}\boldsymbol{\chi}^*_{k|k-1} & \boldsymbol{S}_{Q,k-1}\end{array}\right]\right) \quad (6)$$

where

$$\boldsymbol{Q}_{k-1} = \boldsymbol{S}_{Q,k-1}\boldsymbol{S}^T_{Q,k-1} \quad (7)$$

$$\boldsymbol{\chi}^*_{k|k-1} = \frac{1}{\sqrt{m}}\left[\boldsymbol{X}^*_{1,k|k-1} - \hat{\boldsymbol{X}}_{k|k-1}\boldsymbol{X}^*_{2,k|k-1} - \hat{\boldsymbol{X}}_{k|k-1}\cdots\boldsymbol{X}^*_{m,k|k-1} - \hat{\boldsymbol{X}}_{k|k-1}\right] \quad (8)$$

$Tria\,(\cdot)$ indicates the QR decomposition of the matrix.

Step 3: Measurement update

Evaluate the cubature points $(i = 1, 2, \cdots, m)$

$$\boldsymbol{X}_{i,k|k-1} = \boldsymbol{S}_{k|k-1}\boldsymbol{\xi}_i + \hat{\boldsymbol{X}}_{k|k-1} \quad (9)$$

Evaluate the propagated cubature points

$$\boldsymbol{Z}_{i,k|k-1} = \boldsymbol{h}\left(\boldsymbol{X}_{i,k|k-1}\right) \quad (10)$$

Estimate the measurements

$$\hat{\boldsymbol{Z}}_{k|k-1} = \sum_{i=1}^{m} \omega_i \boldsymbol{Z}_{i,k|k-1} \quad (11)$$

Evaluate the state error variance matrix square root

$$\boldsymbol{S}_{\boldsymbol{Z}\boldsymbol{Z},k|k-1} = Tria\left(\left[\begin{array}{cc}\boldsymbol{\eta}_{k|k-1} & \boldsymbol{S}_{\boldsymbol{R},k}\end{array}\right]\right) \quad (12)$$

where

$$\boldsymbol{R}_k = \boldsymbol{S}_{\boldsymbol{R},k}\boldsymbol{S}^T_{\boldsymbol{R},k} \quad (13)$$

$$\boldsymbol{\eta}_{k|k-1} = \frac{1}{\sqrt{m}}\left[\boldsymbol{Z}_{1,k|k-1} - \hat{\boldsymbol{Z}}_{k|k-1}\boldsymbol{Z}_{2,k|k-1} - \hat{\boldsymbol{Z}}_{k|k-1}\cdots\boldsymbol{Z}_{m,k|k-1} - \hat{\boldsymbol{Z}}_{k|k-1}\right] \quad (14)$$

Calculate the cross covariance matrix

$$\boldsymbol{P}_{\boldsymbol{X}\boldsymbol{Z},k|k-1} = \boldsymbol{\chi}_{k|k-1}\boldsymbol{\eta}^T_{k|k-1} \quad (15)$$

Determine the Kalman gain

$$\boldsymbol{K}_k = \left(\boldsymbol{P}_{\boldsymbol{X}\boldsymbol{Z},k|k-1}/\boldsymbol{S}^T_{\boldsymbol{Z}\boldsymbol{Z},k|k-1}\right)\boldsymbol{S}_{\boldsymbol{Z}\boldsymbol{Z},k|k-1} \quad (16)$$

Update the state value

$$\hat{\boldsymbol{X}}_k = \hat{\boldsymbol{X}}_{k|k-1} + \boldsymbol{K}_k\left(\boldsymbol{Z}_k - \hat{\boldsymbol{Z}}_{k|k-1}\right) \quad (17)$$

Update the state covariance square root

$$\boldsymbol{S}_k = Tria\left(\left[\begin{array}{cc}\boldsymbol{\chi}_{k|k-1} - \boldsymbol{K}_k\boldsymbol{\eta}_{k|k-1} & \boldsymbol{K}_k\boldsymbol{S}_{\boldsymbol{R},k}\end{array}\right]\right) \quad (18)$$

III. IMM-SRCKF ALGORITHM

The IMM algorithm is a tracking algorithm based on the generalized pseudo-Bayesian algorithm, using the Markov probability matrix to accurately switch from one model to another. This algorithm was designed as a model set that contains a finite number of different types of motion submodels, each of which has a corresponding filter. Each filter operates in parallel, and the models are switched between one another by Markov chains. During the tracking process, the system will judge the matching degree between the model and the current target maneuver according to the probability of each model being assigned. The matching degree with the actual target maneuver is higher when the model probability is greater, and vice versa. Furthermore, the interactive operation between models is performed according to this principle, and finally, the outputted results of the estimated values of all of the submodels are fused. Because the algorithm does not need to detect the target maneuver and has a certain self-adjustment, it has a better tracking effect in maneuvering target tracking. Fig. 1 presents a schematic diagram of the IMM algorithm for the multimodel.

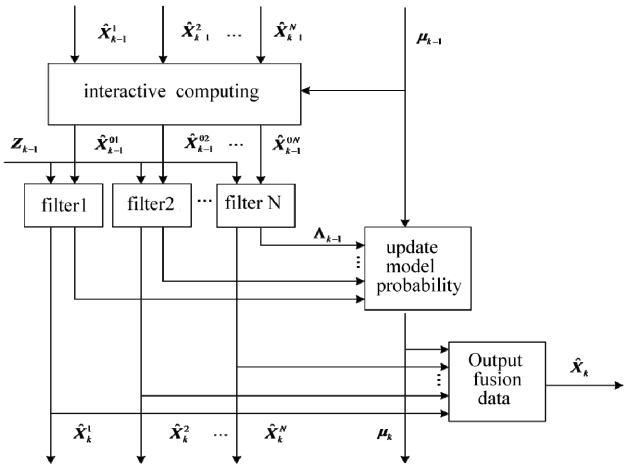

FIGURE 1. IMM-SRCKF algorithm flow chart.

The steps of the IMM algorithm are summarized as follows:

Step 1 **Input interaction**

Let us consider N tracking models. When the motion match model is M_{k-1}^{i} at time $k-1$ and M_k^j at time k, the model mixed probability is $\mu_{k-1}^{i/j}$, which is defined as follows:

$$\begin{aligned}\mu_{k-1}^{i/j} &= P\left(M_{k-1}^{i}/M_k^j, \mathbf{Z}_{k-1}\right)\\ &= \frac{1}{\bar{c}^j}P\left(M_k^j/M_{k-1}^{i}, \mathbf{Z}_{k-1}\right)P\left(M_{k-1}^{i}/\mathbf{Z}_{k-1}\right)\\ &= \frac{1}{\bar{c}^j}p_{ij}\mu_{k-1}^{i}, \quad i,j=1,\cdots N\end{aligned} \tag{19}$$

where p_{ij} represents the Markov transition probability of the model from i to k at time $k-1$, μ_{k-1}^{i} represents the probability of model i as the matching model at time $k-1$, and $\bar{c}^j$ is a normalized constant as follows:

$$\bar{c}^j = \sum_{i=1}^{N} p_{ij}\mu_{k-1}^{i}, \quad j=1,\cdots N \tag{20}$$

Step 2 **Mode interaction**

Using the initial estimate $\hat{\boldsymbol{X}}_{k-1}^{i}$ of the model i to calculate the initial condition of the model j

$$\begin{aligned}\hat{\boldsymbol{X}}_{k-1}^{0j} &= E\left(\boldsymbol{X}_{k-1}|M_k^j, \mathbf{Z}_{k-1}\right)\\ &= \sum_{i=1}^{N}\hat{\boldsymbol{X}}_{k-1}^{i}\mu_{k-1}^{i/j}, \quad i,j=1,\cdots N\end{aligned} \tag{21}$$

$$\begin{aligned}\boldsymbol{P}_{k-1}^{0j} = \sum_{i=1}^{N}\mu_{k-1}^{i/j}\Big[&\boldsymbol{P}_{k-1}^{i} + \left(\hat{\boldsymbol{X}}_{k-1}^{i} - \hat{\boldsymbol{X}}_{k-1}^{0j}\right)\\ &\times\left(\hat{\boldsymbol{X}}_{k-1}^{i} - \hat{\boldsymbol{X}}_{k-1}^{0j}\right)^{T}\Big], \quad i,j=1,\cdots N\end{aligned} \tag{22}$$

Step 3 **Model filter**

$\hat{\boldsymbol{X}}_{k-1}^{0j}$ and $\boldsymbol{P}_{k-1}^{0j}$ obtained in step 2 are used as the initial inputs and are combined with the specific measurement $\boldsymbol{Z}_k$ to filter $j = 1,\cdots N$ parallel models. The estimates of the corresponding state and error covariance matrix are $\hat{\boldsymbol{X}}_k^j$ and $\boldsymbol{P}_k^j$, respectively. The commonly used filter algorithms are EKF, UKF, CKF, etc.; here, the SRCKF algorithm is used.

Step 4 **Update model probability**

a) Calculate the likelihood of the jth model

$$\begin{aligned}\Lambda_k^j &= P\left(\boldsymbol{Z}_k/M_k^j, \boldsymbol{Z}^{k-1}\right) = N\left[\boldsymbol{\gamma}_k^j : 0, \boldsymbol{S}_k^j\right]\\ &= \frac{1}{\sqrt{\left|2\pi\boldsymbol{S}_k^j\right|}}\exp\left[-\frac{1}{2}\left(\boldsymbol{\gamma}_k^j\right)^T\left(\boldsymbol{S}_k^j\right)^{-1}\left(\boldsymbol{\gamma}_k^j\right)\right]\end{aligned} \tag{23}$$

where the residual covariance matrix $\boldsymbol{S}_k^j = \boldsymbol{P}_{zz,k|k-1}$

b) Calculate the condition probability

$$\mu_k^j = P\left(M_k^j/\boldsymbol{Z}^k\right) = \frac{1}{c}\Lambda_k^j\bar{c}^j \tag{24}$$

where $c = \sum_{j=1}^{N}\Lambda_k^j\bar{c}^j$ is a naturalization constant.

Step 5 **Output interaction**

$$\hat{\boldsymbol{X}}_k = \sum_{j=1}^{N}\hat{\boldsymbol{X}}_k^j\mu_k^j \tag{25}$$

$$\begin{aligned}\boldsymbol{P}_k = \sum_{j=1}^{N}\mu_k^j\Big[&\boldsymbol{P}_k^j + \left(\hat{\boldsymbol{X}}_k^j - \hat{\boldsymbol{X}}_k\right)\\ &\times\left(\hat{\boldsymbol{X}}_k^j - \hat{\boldsymbol{X}}_k\right)^T\Big], \quad j=1,\cdots N\end{aligned} \tag{26}$$

IV. ADAPTIVE STSRCKF ALGORITHM

The SRCKF algorithm has a simple structure and high tracking precision, but its ability to adapt to sudden changes in the maneuvering target state is poor. This paper combines the algorithm with the STF and proposes the STSRCKF algorithm. The main idea of the algorithm is to introduce a fading factor into the square root of the state prediction error variance matrix of the SRCKF algorithm, dynamically adjust the gain matrix and compel the output residual sequences to be orthogonal to one another, to extract as much useful information as possible from the residual, and further improve the adaptive tracking ability of the algorithm.

To overcome the poor stability of the EKF algorithm for an uncertain model, the UKF combined with the STF algorithm in [21] is used. It is noted that the filter has strong tracking characteristics; thus, the following two conditions must be satisfied:

1. $E\left[\left(\boldsymbol{X}_k - \hat{\boldsymbol{X}}_k\right)\left(\boldsymbol{X}_k - \hat{\boldsymbol{X}}_k\right)^T\right] = \min$
2. $E\left(\boldsymbol{\gamma}_{k+j}\boldsymbol{\gamma}_k^T\right) = 0 \quad k = 0, 1, 2\ldots, \; j = 1, 2, \ldots$

where γ_{k+j} represents the output residual. case 1 is the index for which the filter achieves the optimal estimation performance, which is the optimal estimate with the minimum mean square error. Orthogonality is required by case 2, which means that the output residual sequences at different times must be kept orthogonal [22].

The principle of orthogonality has been described in detail. When a system model is in a stable state, the output residual should be a white Gaussian noise sequence that is statistically independent under optimal filtering.

$$\boldsymbol{G} = E\left(\boldsymbol{\gamma}_{k+j}\boldsymbol{\gamma}_k^T\right) = \boldsymbol{0}, \quad k = 0, 1, 2\ldots, \; j = 1, 2, \ldots \tag{27}$$

where

$$\boldsymbol{G}_{0,k} = E\left(\gamma_k \gamma_k^T\right) = \boldsymbol{H}_k \boldsymbol{P}_{k|k-1}\boldsymbol{H}_k^T + R_k \tag{28}$$

Q will increase when the state of the system changes suddenly as follows:

$$\boldsymbol{G}_{0,k} > \boldsymbol{H}_k \boldsymbol{P}_{k|k-1}\boldsymbol{H}_k^T + R_k \tag{29}$$

The strong tracking filter solves the above formula, which aims to increase the error covariance prediction matrix, forcing the residual sequence of the output to be orthogonal. Hence, the left and right sides of the inequality are equal, thus suppressing the filter divergence.

$$\boldsymbol{G}_{0,k} = \boldsymbol{H}_k\left(\lambda_k \boldsymbol{F}_k \boldsymbol{P}_{k|k-1}\boldsymbol{F}_k^T + \boldsymbol{Q}_{k-1}\right)\boldsymbol{H}_k^T + R_k \tag{30}$$

A time-varying fading factor λ_{k+1} is introduced in the equation, and $\boldsymbol{P}_{k+1|k}$ is multiplied by λ_{k+1} to ensure the optimality of the filter.

In previous engineering applications, the STF primarily uses a time-varying suboptimal fading factor to reduce the influence of the previous time point on the current filter and to make the current filter value more time-sensitive. The selection method is generally as follows:

$$\lambda_k = \begin{cases} c_k, & c_k > 1 \\ 1, & c_k \le 1 \end{cases}, \; c_k = \frac{tr\left[\boldsymbol{N}_k\right]}{tr\left[\boldsymbol{M}_k\right]} \tag{31}$$

$$\boldsymbol{N}_k = \boldsymbol{G}_k - \beta \boldsymbol{R}_k - \boldsymbol{H}_k \boldsymbol{Q}_{k-1}\boldsymbol{H}_k^T \tag{32}$$

$$\boldsymbol{M}_k = \boldsymbol{H}_k \boldsymbol{\Phi} \boldsymbol{P}_k \boldsymbol{\Phi}^T \boldsymbol{H}_k^T \tag{33}$$

where $tr\left[\cdot\right]$ represents the operand of the matrix trace and $\beta \ge 1$ is a fading factor, which is intended to make the state estimation smoother. The value of the fading factor can be selected empirically. DH Zhou et al. studied the specific value of the filter and proved that when the measurement dimension is more than 5, a β value of 3 can ensure the optimal filtering effect [23]. $\boldsymbol{H}_k$ is a linearized matrix of the measurement equation, which can be obtained by solving the Jacobian matrix, and $\boldsymbol{G}_k$ is the covariance of the actual output residual sequence, which can be obtained by the following approximation.

$$\boldsymbol{G}_k = \begin{cases} \boldsymbol{\gamma}_1 \boldsymbol{\gamma}_1^T, & k = 1 \\ \dfrac{\rho \boldsymbol{G}_{k-1} + \boldsymbol{\gamma}_k \boldsymbol{\gamma}_k^T}{1+\rho}, & k > 1 \end{cases} \tag{34}$$

where $\gamma 1$ is the theoretical output residual sequence; according to [24], $0 < \rho \le 1$ is the forgetting factor and is usually given as $\rho = 0.95$.

According to the above description, the traditional method for obtaining the fading factor is based on the EKF algorithm; thus, the complicated Jacobian matrix $\boldsymbol{H}_k$ needs to be calculated. The SRCKF algorithm is a quadrature Gaussian filter algorithm, and the measurement matrix $\boldsymbol{H}_k$ is not determined in the calculation process; hence, it cannot be directly obtained by the algorithm, and the method of the fading factor cannot be directly applied to the SRCKF. Therefore, to avoid solving the Jacobian matrix, a new method for finding the fading factor under the SRCKF algorithm is derived.

With $\boldsymbol{P}_{k|k-1}^{(l)}$, $\boldsymbol{P}_{zz,k|k-1}^{(l)}$, and $\boldsymbol{P}_{xz,k|k-1}^{(l)}$ as the state prediction covariance matrix, the output prediction covariance matrix and the cross covariance matrix before the time-varying fading factor is introduced, respectively, so obtain

$$\boldsymbol{P}_{k|k-1}^{(l)} = E\left[\left(\boldsymbol{X}_k - \hat{\boldsymbol{X}}_{k|k-1}\right)\left(\boldsymbol{X}_k - \hat{\boldsymbol{X}}_{k|k-1}\right)^T\right] \tag{35}$$

$$\begin{aligned} \boldsymbol{P}_{\boldsymbol{ZZ},k|k-1}^{(l)} &= E\left[\left(\boldsymbol{Z}_k - \hat{\boldsymbol{Z}}_{k|k-1}\right)\left(\boldsymbol{Z}_k - \hat{\boldsymbol{Z}}_{k|k-1}\right)^T\right] \\ &= \boldsymbol{H}_k E\left[\left(\boldsymbol{X}_k - \hat{\boldsymbol{X}}_{k|k-1}\right)\left(\boldsymbol{X}_k - \hat{\boldsymbol{X}}_{k|k-1}\right)^T\right]\boldsymbol{H}_k^T \\ &= \boldsymbol{H}_k \boldsymbol{P}_{k|k-1}^{(l)} \boldsymbol{H}_k^T \end{aligned} \tag{36}$$

$$\begin{aligned} \boldsymbol{P}_{\boldsymbol{XZ},k|k-1}^{(l)} &= E\left[\left(\boldsymbol{X}_k - \hat{\boldsymbol{X}}_{k|k-1}\right)\left(\boldsymbol{Z}_k - \hat{\boldsymbol{Z}}_{k|k-1}\right)^T\right] \\ &= E\left[\left(\boldsymbol{X}_k - \hat{\boldsymbol{X}}_{k|k-1}\right)\left(\boldsymbol{X}_k - \hat{\boldsymbol{X}}_{k|k-1}\right)^T\right]\boldsymbol{H}_k^T \\ &= \boldsymbol{P}_{k|k-1}^{(l)} \boldsymbol{H}_k^T \end{aligned} \tag{37}$$

(37) transforms into

$$\boldsymbol{H}_k = \left[\left(\boldsymbol{P}_{k|k-1}^{(l)}\right)^{-1} \boldsymbol{P}_{\boldsymbol{XZ},k|k-1}^{(l)}\right]^T = \left(\boldsymbol{P}_{k|k-1}^{(l)}\right)^{-1}\left(\boldsymbol{P}_{\boldsymbol{XZ},k|k-1}^{(l)}\right)^T \tag{38}$$

Substituting (38) into (39), (40) is

$$\begin{aligned} \boldsymbol{N}_k &= \boldsymbol{G}_k - \beta \boldsymbol{R}_k - \boldsymbol{H}_k \boldsymbol{Q}_{k-1}\boldsymbol{H}_k^T \\ &= \boldsymbol{G}_k - \beta \boldsymbol{R}_k - \left(\boldsymbol{P}_{\boldsymbol{XZ},k|k-1}^{(l)}\right)^T\left(\boldsymbol{P}_{k|k-1}^{(l)}\right)^{-1} \\ &\quad \times \boldsymbol{Q}_{k-1}\left(\boldsymbol{P}_{k|k-1}^{(l)}\right)^{-1} \boldsymbol{P}_{\boldsymbol{XZ},k|k-1}^{(l)} \end{aligned} \tag{39}$$

$$\begin{aligned} \boldsymbol{M}_k &= \boldsymbol{H}_k \boldsymbol{\Phi} \boldsymbol{P}_k \boldsymbol{\Phi}^T \boldsymbol{H}_k^T \\ &= \boldsymbol{H}_k\left(\boldsymbol{P}_{k|k-1}^{(l)} - \boldsymbol{Q}_{k-1}\right)\boldsymbol{H}_k^T \\ &= \boldsymbol{H}_k \boldsymbol{P}_{k|k-1}^{(l)} \boldsymbol{H}_k^T - \boldsymbol{H}_k \boldsymbol{Q}_{k-1}\boldsymbol{H}_k^T \\ &= \boldsymbol{H}_k \boldsymbol{P}_{k|k-1}^{(l)} \boldsymbol{H}_k^T + \boldsymbol{N}_k - \boldsymbol{G}_k + \beta \boldsymbol{R}_k \\ &= \boldsymbol{P}_{\boldsymbol{ZZ},k|k-1}^{(l)} - \boldsymbol{R}_k + \boldsymbol{N}_k - \boldsymbol{G}_k + \beta \boldsymbol{R}_k \\ &= \boldsymbol{P}_{\boldsymbol{ZZ},k|k-1}^{(l)} + \boldsymbol{N}_k - \boldsymbol{G}_k - (1-\beta)\boldsymbol{R}_k \end{aligned} \tag{40}$$

Since the SRCKF algorithm introduces the idea of matrix QR decomposition, the state prediction covariance matrix $\boldsymbol{P}_{k|k-1}^{(l)}$ and the output prediction covariance matrix $\boldsymbol{P}_{\boldsymbol{ZZ},k|k-1}^{(l)}$ in the above equation are calculated by the their corresponding square roots $\boldsymbol{S}_{k|k-1}^{(l)}$ and $\boldsymbol{S}_{\boldsymbol{ZZ},k|k-1}^{(l)}$:.

$$\boldsymbol{P}_{k|k-1}^{(l)} = \boldsymbol{S}_{k|k-1}^{(l)} \boldsymbol{S}_{k|k-1}^{(l)\,T} \tag{41}$$

$$\boldsymbol{P}_{\boldsymbol{ZZ},k|k-1}^{(l)} = \boldsymbol{S}_{\boldsymbol{ZZ},k|k-1}^{(l)} \boldsymbol{S}_{\boldsymbol{ZZ},k|k-1}^{(l)\,T} \tag{42}$$

Under the SRCKF algorithm, $\boldsymbol{N}_k$ and $\boldsymbol{M}_k$ are expressed as follows:

$$\boldsymbol{N}_k = \boldsymbol{G}_k - \beta \boldsymbol{R}_k - \left(\boldsymbol{P}^{(l)}_{\boldsymbol{XZ},k|k-1}\right)^T \left(\boldsymbol{S}^{(l)}_{k|k-1}\boldsymbol{S}^{(l)}_{k|k-1}{}^T\right)^{-1} \cdot \boldsymbol{Q}_{k-1}\left(\boldsymbol{S}^{(l)}_{k|k-1}\boldsymbol{S}^{(l)}_{k|k-1}{}^T\right)^{-1}\boldsymbol{P}^{(l)}_{\boldsymbol{XZ},k|k-1} \quad (43)$$

$$\boldsymbol{M}_k = \boldsymbol{S}^{(l)}_{\boldsymbol{ZZ},k|k-1}\boldsymbol{S}^{(l)}_{\boldsymbol{ZZ},k|k-1}{}^T + \boldsymbol{N}_k - \boldsymbol{G}_k - (1-\beta)\boldsymbol{R}_k \quad (44)$$

Given $\boldsymbol{P}^{(l)}_{k|k-1}$, $\boldsymbol{P}^{(l)}_{\boldsymbol{ZZ},k|k-1}$, and $\boldsymbol{P}^{(l)}_{\boldsymbol{XZ},k|k-1}$, the time-varying fading factor can be obtained by expressions (41), (42), (43) and (44) under the SRCKF algorithm.

V. MODIFIED MARKOV PROBABILITY MATRIX

According to the IMM algorithm analysis, if the probability of a motion submodel is greater at a certain moment, the matching degree between the model and the real motion pattern of the target is higher; thereby, the probability of the other submodels moving towards this model is greater. For the Nth motion submodel, if the conditional probabilities of submodel j at time $k-1$ and k are μ^j_{k-1} and μ^j_k, respectively, then the probability difference $\left(\mu^j_k - \mu^j_{k-1}\right)$ of the model at consecutive time points directly reflects the change in matching degree between the model and the real moving target. Thus, this paper uses this posterior information to correct the transition probability between models. Due to the nonnegativity of the transfer probability value, and considering the nonnegative monotonicity of the exponential function,

$$\zeta^j_k = e^{\left(\mu^j_k - \mu^j_{k-1}\right)}, \quad j = 1, \cdots N \quad (45)$$

where ζ^j_k represents the probability change rate of model j. $\zeta^j_k > 1$ when the model j probability becomes larger $\left(\mu^j_k - \mu^j_{k-1}\right) > 1$. Similarly, when the probability of the model decreases or remains constant, the corresponding probability change rate is $\zeta^j_k < 1$ or $\zeta^j_k = 1$, respectively. Therefore, ζ^j_k can be used as the correction coefficient of each element in the transition probability matrix to complete the adaptive adjustment of the transition probability as follows:

$$\tilde{p}_{ij,k} = \zeta^j_k \cdot p_{ij,k-1}, \quad i,j = 1, \cdots N \quad (46)$$

where $p_{ij,k-1}$ represents the row i and column j element of the transition probability matrix at time $k-1$ and $\tilde{p}_{ij,k}$ represents the transition probability at the modified time k. At the same time, the elements in the transition probability matrix are nonnegative, and the sum of all elements in each row is equal to 1 due to the properties of time-homogeneous Markov chains.

$$\begin{cases} 0 \le p_{ij} \le 1, \quad i,j = 1, \cdots N \\ \sum_{j=1}^{N} p_{ij} = 1 \end{cases} \quad (47)$$

where $\tilde{p}^{ij}_k$ is normalized as follows:

$$p_{ij,k} = \frac{\tilde{p}_{ij,k}}{\sum_{j=1}^{N}\tilde{p}_{ij,k}} = \frac{\zeta^j_k \cdot p_{ij,k-1}}{\sum_{j=1}^{N}\zeta^j_k \cdot p_{ij,k-1}} = \frac{e^{\left(\mu^j_k - \mu^j_{k-1}\right)}p_{ij,k-1}}{\sum_{j=1}^{N} e^{\left(\mu^j_k - \mu^j_{k-1}\right)}p_{ij,k-1}} \quad (48)$$

where $p_{ij,k}$ represents the transfer probability of the final-modified moment k. According to (48), if the probability of submodel j increases at time k, the j column element p^{ij}_k of the modified transition probability matrix also increases; thus, the proportion of model j as the matching model in the filtering estimation will further increase in the model mixed interaction of the next algorithm time point. Conversely, p^{ij}_k decreases and the proportion of model j as a nonmatching model in the filter estimation will be further reduced when the probability of submodel j decreases at time k. Therefore, this online real-time adjustment of the model transfer probability can restrict the use of nonmatched information while expanding the advantages of matching information. In model switching, the role of the matching model is increased, while the influence of the nonmatching model is reduced, and the switching speed and filtering accuracy of the algorithm model are improved.

VI. EXPERIMENTS AND RESULTS

The root mean square error (RMSE) is used to evaluate the tracking results of the algorithms. The position RMSE is defined as follows:

$$RMSE(k) = \sqrt{\frac{1}{M}\sum_{m=1}^{M}\left[(x^m_k - \hat{x}^m_k)^2 + (y^m_k - \hat{y}^m_k)^2\right]} \quad (49)$$

$$ARMSE = \frac{1}{N}\sum_{n=1}^{N} RMSE(K) \quad (50)$$

where (x^m_k, y^m_k) and $(\hat{x}^m_k, \hat{y}^m_k)$ are the true position coordinates and estimated coordinates of the target at the $k-th$ moment in the $m-th$ simulation, respectively. The speed RMSE can be similarly obtained.

A. MEASUREMENT AND TRACKING MODEL

For target tracking in a two-dimensional plane, the spatial measurement information selects azimuth β_k and its change rate $\dot{\beta}_k$ at time k. The frequency domain measurement information selects the Doppler frequency change rate $\dot{f}_{dk}$ at time k.

$$\beta_k = \arctan\left(\frac{x_k}{y_k}\right) \quad (51)$$

$$\dot{\beta}_k = \frac{\dot{x}_k y_k - x_k \dot{y}_k}{x^2_k + y^2_k} \quad (52)$$

$$\dot{f}_{dk} = -\frac{f_T}{c}\left(r_k \dot{\beta}^2_k\right) = -\frac{f_T\left(\dot{x}_k y_k - x_k \dot{y}_k\right)^2}{c\left(x^2_k + y^2_k\right)^{3/2}} \quad (53)$$

where f_T is the signal frequency emitted by the target, c is the propagation speed of the electromagnetic wave, and the

radial distance between the target and the observation station at time k is $r_k = \sqrt{x_k^2 + y_k^2}$. Let $\boldsymbol{h}(\boldsymbol{X}_k) = \left[\begin{array}{ccc} \beta_k & \dot{\beta}_k & \dot{f}_{dk} \end{array}\right]^T$; then, the system observation equation is as follows:

$$\boldsymbol{Z}_k = \boldsymbol{h}(\boldsymbol{X}_k) + \boldsymbol{V}_k \tag{54}$$

where $\boldsymbol{V}_k = \left[\begin{array}{ccc} \sigma_{\beta_k} & \sigma_{\dot{\beta}_k} & \sigma_{\dot{f}_{dk}} \end{array}\right]^T$ is the observation noise and σ_{β_k}, $\sigma_{\dot{\beta}_k}$ and $\sigma_{\dot{f}_{dk}}$ are the zero, mean and independent white Gaussian noise, respectively, with the covariance matrix $\boldsymbol{R}_k = diag\left[\begin{array}{ccc} \sigma_{\beta_k}^2 & \sigma_{\dot{\beta}_k}^2 & \sigma_{\dot{f}_{dk}}^2 \end{array}\right]$.

In the actual tracking process, target maneuvers are highly dynamic and stochastic, and a single model cannot cover everything. However, each complex maneuver can be regarded as a simple weighting of several models, so it is necessary to establish a basic target model. This paper uses the constant velocity (CV) model and coordinated turn (CT) model to model the target.

Uniform circular motion is also called a CT. With this type of motion, the direction of velocity is constantly changing during the entire process, while the speed and angular velocity remain unchanged. Similarly, taking $\boldsymbol{X} = \boldsymbol{X}_T - \boldsymbol{X}_O = \left[\begin{array}{ccccc} x & \dot{x} & \ddot{x} & y & \dot{y} & \ddot{y} \end{array}\right]^T$ as the state vector, experiment assume that the target radiation source exhibits uniform circular motion in a two-dimensional plane; then, the model state equation can be written as follows:

$$\begin{aligned} \boldsymbol{X}_k &= \boldsymbol{\Phi}\boldsymbol{X}_{k-1} + \boldsymbol{\Gamma}\boldsymbol{w}_{\boldsymbol{k}} \\ &= \begin{bmatrix} 1 & \frac{\sin\omega T}{\omega} & 0 & \frac{\cos\omega T - 1}{\omega} \\ 0 & \cos\omega T & 0 & -\sin\omega T \\ 0 & \frac{1-\cos\omega T}{\omega} & 1 & \frac{\sin\omega T}{\omega} \\ 0 & \sin\omega T & 0 & \cos\omega T \end{bmatrix} \boldsymbol{X}_{k-1} \\ &\quad + \begin{bmatrix} \frac{T^2}{2} & 0 \\ T & 0 \\ 0 & \frac{T^2}{2} \\ 0 & T \end{bmatrix} \boldsymbol{w}_{\boldsymbol{k}} \end{aligned} \tag{55}$$

where ω represents the known turn rate of target movement; $\omega > 0$ represents a left turn, and $\omega < 0$ represents a right turn. $\boldsymbol{w}_k$ is two-dimensional white Gaussian noise with a zero mean. $\boldsymbol{Q}_k = E\left[\boldsymbol{\Gamma}\boldsymbol{w}_k\boldsymbol{w}_k^T\boldsymbol{\Gamma}^T\right]$ is the state noise covariance matrix.

When the system model is the discrete CV model, the relative state vector $\boldsymbol{X}_k = \boldsymbol{X}_{Tk} - \boldsymbol{X}_{Tk} = \left[\begin{array}{ccccc} x_k & \dot{x}_k & \ddot{x}_k & y_k & \dot{y}_k & \ddot{y}_k \end{array}\right]^T$ of the target emitter and the observation platform is taken as the state variable. Therefore, the equation of state of the system can be obtained as follows:

$$\boldsymbol{X}_k = f\left(\boldsymbol{X}_{k-1}\right) + \boldsymbol{\Gamma}\boldsymbol{w}_{\boldsymbol{k}} = \boldsymbol{\Phi}\boldsymbol{X}_{k-1} + \boldsymbol{\Gamma}\boldsymbol{w}_{\boldsymbol{k}} \tag{56}$$

where $\boldsymbol{\Phi} = \begin{bmatrix} \boldsymbol{I}_2 & T\boldsymbol{I}_2 \\ 0\boldsymbol{I}_2 & \boldsymbol{I}_2 \end{bmatrix}$ is the state transition matrix, T is the measurement interval, $\boldsymbol{I}_2$ is the 2×2 identity matrix; $\boldsymbol{\Gamma} = \begin{bmatrix} \frac{T^2}{2}\boldsymbol{I}_2 \\ T\boldsymbol{I}_2 \end{bmatrix}$ is the state noise transfer matrix; $\boldsymbol{w}_k = \left[\begin{array}{cc} w_x & w_y \end{array}\right]^T$ is the system disturbance noise; w_x and w_y are zero-mean and independent white Gaussian noise, respectively; and $\boldsymbol{Q}_k = E\left[\boldsymbol{\Gamma}\boldsymbol{w}_k\boldsymbol{w}_k^T\boldsymbol{\Gamma}^T\right]$ is the state noise covariance matrix.

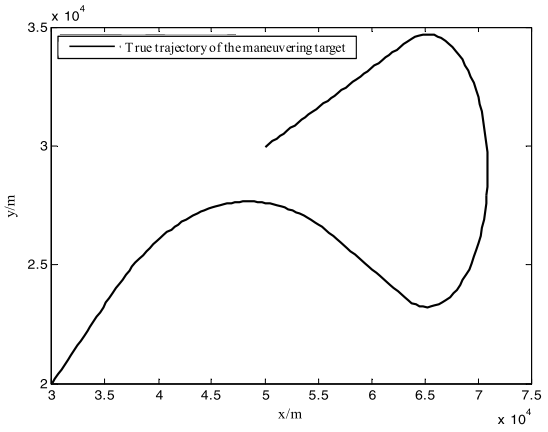

FIGURE 2. True trajectory of the maneuvering target.

B. SIMULATION AND ANALYSIS

To assume that the reconnaissance platform is fixed at the origin (0, 0) of the two-dimensional coordinate system, and the initial state of the target radiation source is $\boldsymbol{X}_0 = [20km\ 180m/s\ 0m/s^2\ 25km\ 200m/s\ 0m/s^2]^T$. Nonmaneuvering, weak maneuvering and strong maneuvering motions of the target are simulated by using two movements of uniform speed and a CT. The specific motion process is uniform linear motion at the initial speed for the first 20 s, a slow, weak turn occurs to the right from 21 s-80 s, with a turning rate of $\omega = 0.9rad/s$, and uniform linear motion is recovered from 81 s-100 s. At t = 101 s, the target makes a strong turn to the left at a turning rate of $\omega = -3.6rad/s$. After 60 s of continuous movement, the movement state changes again at t = 161 s, and the target returns to uniform linear motion until the end of the simulation. Fig. 2 presents the true trajectory of the maneuvering target.

It should be noted that in order to compare the performance of the two algorithms, a discussion of the model set selection is neglected. It is assumed that the selected submodel can completely cover the entire process of movement. One CV model and two CT models with the same turning rate for real motion conditions, CT1 ($\omega = 0.9rad/s$) and CT2 ($\omega = -3.6rad/s$), are employed to describe the actual motion of the target. The initial Markov transition probability matrix is set as $\begin{bmatrix} 0.95 & 0.025 & 0.025 \\ 0.025 & 0.95 & 0.025 \\ 0.025 & 0.025 & 0.95 \end{bmatrix}$; the initial probability of each submodel is [0.2, 0.4, 0.4], for which the CV model probability is 0.2; the initial value of the state error covariance matrix $\boldsymbol{P}_0 = diag[500050]$; the observation period is $T = 1s$; the observation time is $N = 200s$; the target radiation frequency is $f_T = 10GHz$; and the measurement accuracy of the azimuth angle, azimuth angle change rate and Doppler

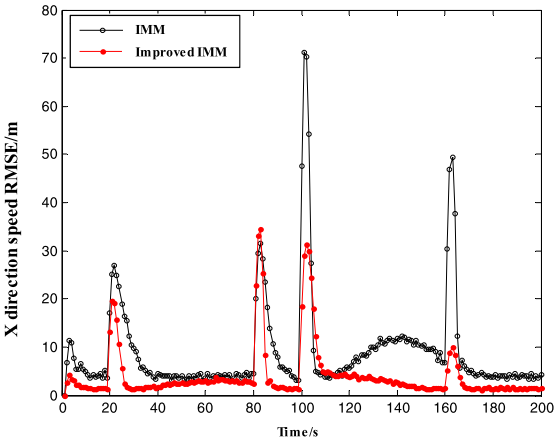

FIGURE 3. Comparison of the velocity RMSE in the X direction.

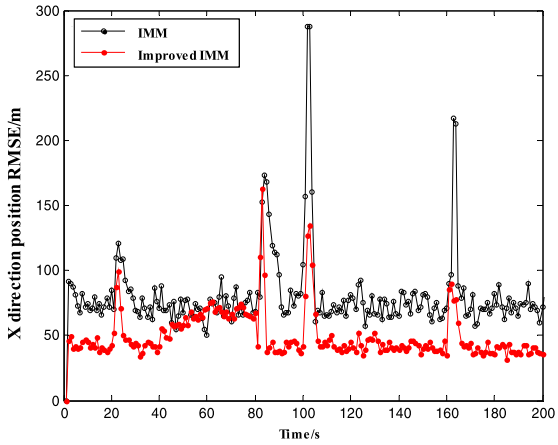

FIGURE 4. Comparison of the position RMSE in the X direction.

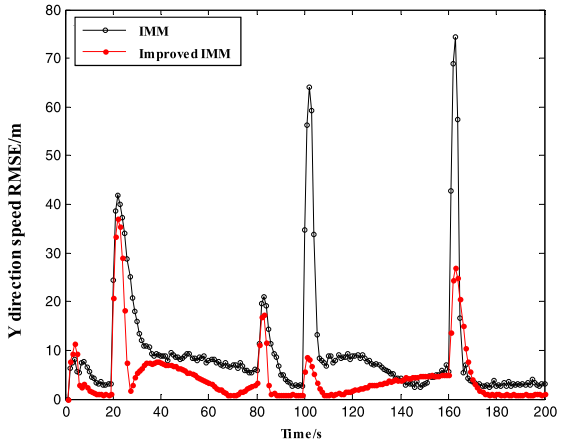

FIGURE 5. Comparison of the velocity RMSE in the Y direction.

frequency change rate are $10mrad$, $0.2mrad/s$ and $0.6Hz/s$, respectively.

The simulation results in Fig. 3∼Fig. 6 show that the improved IMM algorithm has a higher tracking accuracy throughout the entire motion process. Compared with nonmaneuver and weak maneuver motion, the improved algorithm

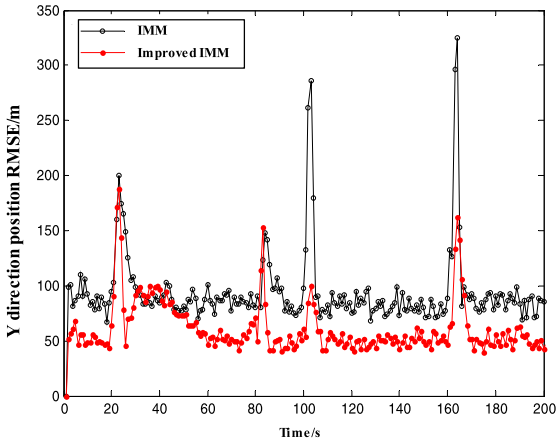

FIGURE 6. Comparison of the position RMSE in the Y direction.

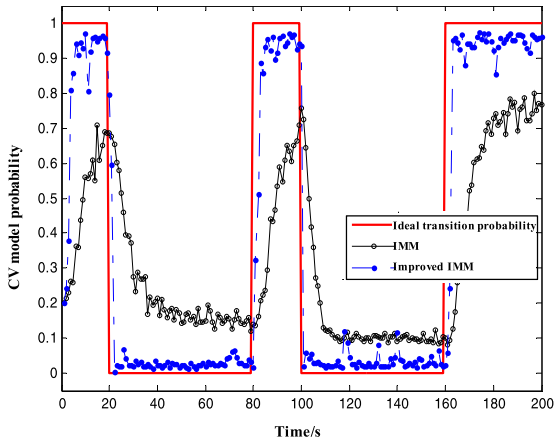

FIGURE 7. Comparison of the CV model probability curves.

has more tracking advantages during abrupt maneuvering mutation. From the perspective of the filter algorithm, these results occur because the covariance of the actual output residual sequence of the STSRCKF algorithm is extremely small in the nonmaneuver and weak maneuver cases, causing the time-varying fading factor to approach 1, which leads the STSRCKF algorithm to degenerate into the standard SRCKF algorithm. However, the advantages of the fading factor in the STSRCKF algorithm can be fully reflected when a strong maneuver leads to a rapid increase in the filtering residual. In the algorithm, the dynamic change of the fading factor increases with an increase in the predicted residual, and the square root of the error covariance is adjusted online. Then, the gain matrices of the system are adjusted to one another, and the residual sequences are forced to be orthogonal to one another; thus, the system's adaptive tracking and tracking performance abilities are improved.

From Fig. 7∼ Fig. 9, it can be seen that the improved IMM algorithm is more reasonable in the allocation of each submodel, with a faster switching speed. When the four target states of 21 s, 81 s, 101 s and 161 s change, the original algorithm model has a slow switching speed, and the three

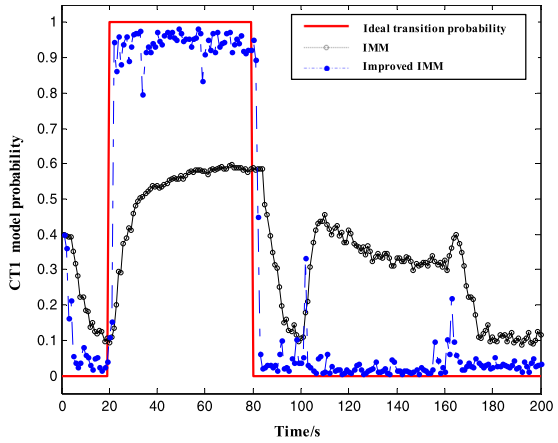

FIGURE 8. Comparison of the CT1 model probability curves.

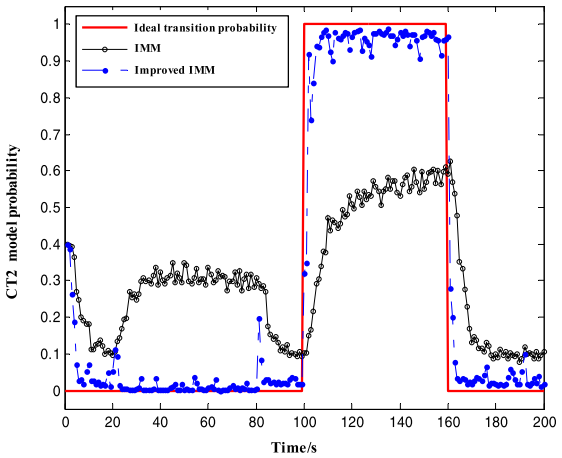

FIGURE 9. Comparison of the CT2 model probability curves.

submodels have a large difference from the ideal transition probability curve; thus, the matching degree with the real model is low. In comparison, the improved IMM algorithm makes full use of the posterior information of the conditional probability difference and can quickly switch to match the real motion when the state changes, thus completing the rational allocation of different submodels and making the probability curves of each model very close to the ideal transition probability curve. Therefore, the tracking effect of the improved IMM algorithm is superior.

To more fully illustrate the advantages of the IIMM-STSRCKF algorithm. The algorithm is compared to the standard IMM, STSRCKF, STCKF and STFQM. Table 1 shows the SRMSE values of the filter. The accuracy of IIMM-STSRCKF is significantly improved and the tracking stability is relatively stable. STSRCKF is better that SRCKF in accuracy and stability. these findings suggest that the strong tracking filter has a good effect on complex maneuvering target. The equivalent solution method of the new time-varying fading factor improves the filtering precision of the IMM algorithm.

TABLE 1. ARMSE for position and acceleration.

Performance (ARMSE)	X-position (m)	Y-position (m)	X-velocity (m/s)	Y-velocity (m/s)
Standard IMM	8.4	68.6	7.9	88.7
STSRCKF	10.5	80.4	12.4	80.3
IIMM-STSRCKF	4.2	48	5.1	50.3
SRCKF	15.7	72.1	8.5	87.4
STFQM	9.3	70.1	6.9	60.3

VII. CONCLUSIONS

In this paper, an IIMM–STSRCKF algorithm is proposed for complex strong maneuvers. Based on the IMM, this algorithm uses strong tracking to deduce a new equivalent method for evaluating the time-varying fading factor, which is introduced into the square root of the state error covariance matrix of the SRCKF algorithm, thus giving the STSRCKF algorithm the ability to track strong maneuvers. Furthermore, adaptive adjustment of the Markov probability transfer matrix is achieved by using the probability difference between two consecutive time points in the IMM algorithm, which improves the switching speed and the rationality of the submodel. Compared with the traditional IMM algorithm model, the IIMM-STSRCKF algorithm exhibits greatly improved tracking accuracy, model switching speed and computation. Methods for further improving the real-time performance of the algorithm for tracking complex maneuvering targets will be investigated in future research.

REFERENCES

[1] Y. Li *et al.*, "A passive detection and tracking divers method based on energy detection and EKF algorithm," in *Cluster Computing*, vol. 7. Sep. 2017, pp. 1–10.

[2] W. Zhu, W. Wang, and G. Yuan, "An improved interacting multiple model filtering algorithm based on the cubature Kalman filter for maneuvering target tracking," *Sensors*, vol. 16, no. 6, p. 805, Jun. 2016.

[3] F. Masoumi-Ganjgah, R. Fatemi-Mofrad, and N. Ghadimi, "Target tracking with fast adaptive revisit time based on steady state IMM filter," *Digit. Signal Process.*, vol. 69, pp. 154–161, Oct. 2017.

[4] S. Vasuhi and V. Vaidehi, "Target tracking using interactive multiple model for wireless sensor network," *Inf. Fusion*, vol. 27, pp. 41–53, Jan. 2016.

[5] B. Jia *et al.*, "Space object tracking and maneuver detection via interacting multiple model cubature Kalman filters," presented at the IEEE Aerosp. Conf., Big Sky, MT, USA, Mar. 2015, pp. 1–8.

[6] R. Marino, "Adaptive observers for single output nonlinear systems," *IEEE Trans. Autom. Control*, vol. 35, no. 9, pp. 1054–1058, Sep. 1990.

[7] C.-Y. Yang, B.-S. Chen, and F.-L. Liao, "Mobile location estimation using fuzzy-based IMM and data fusion," *IEEE Trans. Mobile Comupt.*, vol. 9, no. 10, pp. 1424–1436, Oct. 2010.

[8] I. Hwang, C. E. Seah, and S. Lee, "A study on stability of the interacting multiple model algorithm," *IEEE Trans. Autom. Control*, vol. 62, no. 2, pp. 901–906, Feb. 2017.

[9] W. Li and Y. Jia, "Location of mobile station with maneuvers using an IMM-based cubature Kalman filter," *IEEE Trans. Ind. Electron.*, vol. 59, no. 11, pp. 4338–4348, Nov. 2012.

[10] H.-S. Kim, J. G. Park, and D. Lee, "Adaptive fuzzy IMM algorithm for uncertain target tracking," *Int. J. Control Autom. Syst.*, vol. 7, no. 6, pp. 1001–1008, Jun. 2009.

[11] B.-D. Kim and J.-S. Lee, "IMM algorithm based on the analytic solution of steady state Kalman filter for radar target tracking," presented at the IEEE Int. Radar Conf., Arlington, VA, USA, May 2005.
[12] Q. Shen, "Kurtosis-based IMM filter for multiple MEMS gyroscopes fusion," *Sensor Rev.*, vol. 37, no. 3, Mar. 2017.
[13] Z. Duan and X. Li, "A new nonlinear state estimator using the fusion of multiple extended Kalman filters," presented at the 18th Int. Conf. Inf. Fusion, Washington, DC, USA, Jul. 2015.
[14] A. Katriniok and D. Abel, "Adaptive EKF-based vehicle state estimation with online assessment of local observability," *IEEE Trans. Control Syst. Technol.*, vol. 24, no. 4, pp. 1368–1381, Jul. 2016.
[15] Y. Wang *et al.*, "Dynamic propagation characteristics estimation and tracking based on an EM-EKF algorithm in time-variant MIMO channel," *Inf. Sci.*, vol. 408, pp. 70–83, Oct. 2017.
[16] S. J. Julier and J. K. Uhlmann, "Unscented filtering and nonlinear estimation," *Proc. IEEE*, vol. 92, no. 3, pp. 401–422, Mar. 2004.
[17] I. Arasaratnam and S. Haykin, "Cubature Kalman filters," *IEEE Trans. Autom. Control*, vol. 54, no. 6, pp. 1254–1269, Jun. 2009.
[18] Q. Ge, D. Xu, and C. Wen, "Cubature information filters with correlated noises and their applications in decentralized fusion," *Signal Process.*, vol. 94, pp. 434–444, Jan. 2014.
[19] I. Arasaratnam, S. Haykin, and T. R. Hurd, "Cubature Kalman filtering for continuous-discrete systems: Theory and simulations," *IEEE Trans. Signal Process.*, vol. 58, no. 10, pp. 4977–4993, Oct. 2010.
[20] J. Duan, H. Shi, D. Liu, and H. Yu, "Square root cubature Kalman filter-Kalman filter algorithm for intelligent vehicle position estimate," *Procedia Eng.*, vol. 137, pp. 267–276, 2016.
[21] J. P. Muñoz, M. E. Magaña, and E. Cotilla-Sanchez, "Adaptive master–slave unscented Kalman filter for grid voltage frequency estimation," *IET Signal Process.*, vol. 12, no. 4, pp. 496–505, Jun. 2017.
[22] H. Wang, G. Fu, X. Bian, and J. Li, "SRCKF based simultaneous localization and mapping of mobile robots," *Robot*, vol. 35, no. 2, pp. 200–207, 2013.
[23] X. Tang, Z. Liu, and J. Zhang, "Square-root quaternion cubature Kalman filtering for spacecraft attitude estimation," *Acta Astron.*, vol. 76, no. 4, pp. 84–94, Jul./Aug. 2012.
[24] C. Hai and S. Ganlin, "Attitude angle aided IMMCKF algorithm," presented at the IEEE 10th Int. Conf. Electron. Meas. Instrum., Chengdu, China, Aug. 2011.
[25] A. K. Singh and S. Bhaumik, "Higher degree cubature quadrature kalman filter," *Int. J. Control Autom. Syst.*, vol. 13, no. 5, pp. 1097–1105, Oct. 2015.
[26] B. Jia, M. Xin, and Y. Cheng, "High-degree cubature Kalman filter," *Automatica*, vol. 49, no. 2, pp. 510–518, Feb. 2013.
[27] B. Jia and M. Xin, "Multiple sensor estimation using a new fifth-degree cubature information filter," *Trans. Inst. Meas. Control*, vol. 37, no. 1, pp. 15–24, 2015.
[28] T. Sun and M. Xin, "Multiple UAV target tracking using consensus-based distributed high degree cubature information filter," presented at the AIAA Guid., Navigat., Control Conf., Kissimmee, FL, USA, Jan. 2015.
[29] T. Sun and M. Xin, "Hypersonic entry vehicle state estimation using high degree cubature Kalman filter," presented at the AIAA Atmos. Flight Mech. Conf., Atlanta, GA, USA, Jun. 2014.
[30] B. Jia, M. Xin, and Y. Cheng, "Sparse-grid quadrature nonlinear filtering," *Automatica*, vol. 48, no. 2, pp. 327–341, 2012.
[31] T. Xu, Q. Ge, X. Feng, and C. Wen, "Strong tracking filter with bandwidth constraint for sensor networks," presented at the 18th IEEE Int. Conf. Control Automat., Xiamen, China, Jul. 2010.
[32] S. Ma, P. Wu, J. Ji, and X. Li, "Sensorless control of salient PMSM with adaptive integrator and resistance online identification using strong tracking filter," *Int. J. Electron.*, vol. 103, no. 2, pp. 217–231, 2016.
[33] G. Hu, S. Gao, Y. Zhong, B. Gao, and A. Subic, "Modified strong tracking unscented Kalman filter for nonlinear state estimation with process model uncertainty," *Int. J. Control*, vol. 29, no. 12, pp. 1561–1577, Dec. 2015.
[34] D.-J. Jwo and S.-Y. Lai, "Navigation integration using the fuzzy strong tracking unscented Kalman filter," *J. Navigat.*, vol. 62, no. 2, pp. 303–322, Feb. 2009.
[35] W. Li and Q. Ge, "UKF-STF tracking with correlated noises for the nonlinear system," presented at the 8th World Congr. Intell. Control Automat., Jinan, China, Jul. 2010.
[36] X. Li, Z. Xu, and D. Zhou, "Chaotic secure communication based on strong tracking filtering," *Phys. Lett. A*, vol. 372, no. 44, pp. 6627–6632, Oct. 2008.
[37] D. H. Zhou and P. M. Frank, "Strong tracking filtering of nonlinear time-varying stochastic systems with coloured noise: Application to parameter estimation and empirical robustness analysis," *Int. J. Control*, vol. 65, no. 2, pp. 295–307, Feb. 1996.
[38] D.-J. Jwo, C.-F. Yang, C.-H. Chuang, and T.-Y. Lee, "Performance enhancement for ultra-tight GPS/INS integration using a fuzzy adaptive strong tracking unscented Kalman filter," *Nonlinear Dyn.*, vol. 73, no. 1, pp. 377–395, Jul. 2013.

BO HAN was born in Xi'an, China, in 1992. He received the M.S. degree in intelligence testing from the Air Force Engineering University, in 2017. He is currently pursuing the Ph.D. degree in UAV operational engineering. His main research interests are UAV path planning, state prediction, and maneuvering decision-making, especially in high dynamic countermeasure.

HANQIAO HUANG was born in 1982. He received the Ph.D. degree in navigation, guidance and control from Northwestern Polytechnic University, in 2010. He is currently an Associate Professor and holds a postdoctoral position with Northwestern Polytechnical University. His research interest includes optimization algorithms and its application in cooperative combat for unmanned combat aerial vehicle.

LEI LEI was born in 1990. He received the M.S. degree in electrical engineering from Xi'an Jiaotong University, in 2015. He is working in Shanxi Electric Power Company. His research interests include environmental protection, water conservation monitoring, remote sensing, and UAV monitoring.

CHANGQIANG HUANG was born in 1961. He received the Ph.D. degree in navigation, guidance and control from Northwestern Polytechnic University, in 2006. He is currently a Professor and a Doctoral Tutor with Air Force Engineering University. He has worked in aerial weapon system and application engineering for more than 30 years. His current research interests include artificial intelligence, including knowledge extraction and air combat simulation systems.

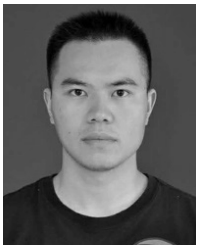

ZHUORAN ZHANG was born in 1990. He received the M.S. degree in unmanned aircraft combat system and technology from Air Force Engineering University, in 2015, where he is currently pursuing the Ph.D. degree. His research interest includes optimization algorithm and its application in unmanother factors are futher slovedned aerial vehicle combat systems.